Crystal adjustment by means of blocking pattern

H. Ellmer,[a] R. Aichinger, E. Winkler, and D. Semrad
Institut für Experimentalphysik, Johannes-Kepler-Universität, A-4040 Linz, Austria

V. Mergel and O. Jagutzki
Institut für Kernphysik, Universität Frankfurt, D-60323 Frankfurt, Germany

(Received 7 June 1999; accepted for publication 5 April 2000)

A facility is described to record the blocking pattern of a single crystal produced by 400 keV protons. By this we aim at a reliable, fast, and careful procedure to align single crystals to the incoming ion beam. The two-dimensional position sensitive detector (2D-PSD) system from Roentdek GmbH Frankfurt/M, Germany, is based on three microchannel plates arranged in a *Z* stack. The essential shortcoming of this detector is its low sensitivity to high energy (>200 keV) projectiles. To reproduce the pattern formed by 400 keV protons on the 2D-PSD we had to decrease their energy to a few tens of kiloelectron-volts by a stopping foil of 3.5 μm Mylar®. This foil has the additional advantage of absorbing slow projectiles and sputtered atoms emerging from the target. On their way to the detector, these slow particles, in case they are charged, would be strongly influenced by electric fields and would thus obscure the true pattern. At present, our facility allows us to routinely align crystals for channeling measurements accurately, fast and, for most applications, with an acceptable amount of radiation damage. © *2000 American Institute of Physics.* [S0034-6748(00)02707-6]

I. INTRODUCTION

For investigation of single crystals, ion beam scattering is still an unrivaled technique in configuration space. As such, it perfectly complements methods that may be best described in momentum space, like x-ray, electron, neutron, and thermal energy atom scattering. Characterization of crystals by ion beams is mainly based on the interpretation of dips in the backscattering yield when low index planes or axes of the crystal are aligned either with the incoming beam (channeling) or with the direction to the detector (blocking) or with both (channeling–blocking).

An essential precondition for these measurements is the knowledge of the accurate angular orientation of the target. Commonly, the target is moved within a certain solid angle so that the set of channeling dips in the backscattering yield clearly defines the angular position of the crystal. The inverse procedure may also be applied: The beam enters the crystal in a random direction and a small detector scans a corresponding solid angle giving the blocking pattern. As a consequence of the rule of reversibility,[1] blocking can be treated the same way as channeling.

The problem is that aligning the target by ions prior to the actual measurement always induces radiation damage to the target that might not be negligible. This contribution deals with an optimization of this aligning procedure. To avoid time-consuming readjustment of the three axes goniometer where the target is mounted we want to obtain all information about the angular orientation from a single measurement with both the target crystal and the detector at fixed angular positions.

[a]Electronic mail: ellmer@exphys.uni-linz.ac.at

II. OPTIMIZATION

First we had to decide between channeling and blocking geometry. In Fig. 1 we show an idealized universal layout where—at least on principle—both procedures can be performed. It is obvious that for channeling (labeled C in the figure) we need a position sensitive detector (PSD) to know for each particle scattered into the detector the direction of flight before hitting the target. This PSD has to be of transmission type and has to manage up to 10^9 projectiles per second. Since these specifications cannot be met by any existing detector we had to confine ourselves to blocking (labeled B in Fig. 1).

To obtain the blocking pattern (also called protonogram, i.e., ionogram with protons) on the PSD, the impact coordinates of the particles scattered from the target have to be determined. We therefore can use a standard PSD and could follow the principle suggested by Fig. 1. However, in general one has no convergent beam to average over a sufficiently large solid angle but a parallel beam at some random direction of the crystal. Following Lindhard[1] one can argue that there should be no essential difference in the result of both layouts. Hence, we tested a commercial two-dimensional position sensitive detector (2D-PSD) for its capability to register blocking patterns obtained with 400 keV protons. The device was intended to be installed and is now installed in the target chamber of our 180° backscattering assembly APIS (Assembly for Π-Scattering[2]) to simplify target adjustment.

There are two sorts of 2D-PSDs available. The optimum solution would be an energy dispersive and position sensitive semiconductor detector.[3] Detectors like these have been used in high energy physics, e.g., to measure fission lifetimes as function of excitation energy.[4] According to the method in

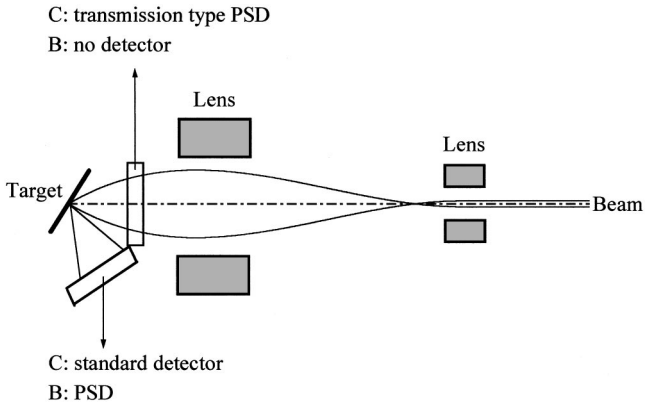

FIG. 1. Idealized experimental layout where both target adjustment by channeling and by blocking can be performed in a single run.

which position information is obtained, we can distinguish essentially two types: the pixel detector where the detector active area is divided in pixels and the pixel pitch size gives the position resolution. These detectors show high energy resolution and manage very high counting rates. However, each pixel cell has to contain a complete signal processing chain. So the essential shortcoming is the large amount of electronics—there might be as many as 288 CMOS readout chips.[5] In contrast, for resistive layer and drift detectors the information is obtained from resistive charge division or from drift time to the electrodes. The most common 2D-PSD in high energy physics employs resistive charge division. For instance, the spatial resolution of a 50×50 mm^2 square detector for 40 MeV He projectiles is 1.4 mm, corresponding to 1225 pixels. However, a scaling law states that the position resolution depends on the inverse of the total energy deposited in the active volume of the detector. In fact, for 400 keV He ions one measures the quite poor spatial resolution of 52 mm,[6] which corresponds formally to 1 pixel. These data apply to an active thickness of 300 μm, resistive active area of 18 000 Ω cm and 1020 pF detector capacitance with four resistive strips each between two corners.

The alternative 2D-PSD is based on microchannel plates (MCPs). To get high amplification either two MCPs are mounted chevron like or three MCPs in a *Z* stack.[7] They are supported by a ceramic disk with a germanium layer on the side facing the MCP and with a position sensitive wedge-and-strip (WS) anode on the other. More details on the construction and on the operating conditions will be discussed in Sec. III. The MCPs are operated at a maximum voltage of 1000 V per unit. As signal processing to get undistorted two-dimensional information is rather delicate it is recommended to operate the assembly with the MCP output side close to ground potential; consequently, the input side of the topmost MCP is negatively charged, in our case to -2700 V.

The most prominent drawback of the MCP is the strong and nonmonotonic energy dependence of its detection efficiency.[8] A maximum of about 85% is found for 2 keV protons. Going down in energy, one finds a threshold[9] at some hundreds of electron volts, depending on the projectile's mass (for 500 eV protons $\epsilon\approx 5\%$). With increasing energy the efficiency ϵ decreases in the first instance slowly (for 50 keV $\epsilon\approx 60\%$) but for still higher energies ϵ goes down rather fast ($\epsilon\approx 4\%$ for 200 keV and $\epsilon<2\%$ for 400 keV). Unfortunately, the blocking dips are best developed for projectiles backscattered near the surface of the crystal so that they have energies close to the primary energy $E_0 = 400$ keV.

We want to show by simple estimates that due to the poor efficiency of the MCPs for fast projectiles and to an electric field acting on the way from the target to the detector, that the layout according to version B of Fig. 1 will not work. In these experiments, the target was a tungsten single crystal with its surface cut parallel to the (111) plane. It is charged to $+130$ V to prevent secondary electrons from leaving the target. The 2D-PSD subtends a solid angle of $\Omega_{\rm det}=0.076$ sr. But due to an electric field extending from the target ($+130$ V) to the input side of the PSD (-2700 V) the effective solid angle for low energy, positively charged particles will be significantly larger. There are two species of particles hitting the detector, backscattered protons or hydrogen atoms and sputtered W atoms or positively charged W^+ ions, respectively. We estimate the magnitude of the individual contributions on the following assumptions. For a 400 keV beam the energies of backscattered projectiles range from 0 to 393 keV and their number is[10] about $N_p\approx 100\times 10^{-6}$ per incoming proton. The backscattering spectrum $n(E)$ is assumed to have a $1/\sqrt{E}$ dependence, not only at low energies[11] but for $0<E<kE_0$, so that

$$n(E)=N_p/(2\sqrt{kE_0E}), \tag{1}$$

with k the kinematic factor. Sputtered target atoms (W) have energies in the electron volt region;[12] their yield per 400 keV proton is[13] about $N_s\approx 2\times 10^{-6}$. Finally, at low energies the fraction of charged particles exiting a ''dirty'' oxidized W surface is[14] $\approx 10\%$ for both W^+ ions and protons.

Now the problem can best be seen when we consider the image on the 2D-PSD as composed of five distributions as follows. (i) High energy projectiles, i.e., protons with energies >200 keV. In brackets we give the approximate probability for an incoming projectile to be either reflected with a given energy or to eject a target particle, both in a given charge state. For example, for this contribution we multiply the backscattering yield of 0.01 with the relative solid angle $\Omega_{\rm rel}=0.076/(2\pi)\approx 0.01$, by 0.29—that is the fraction of the spectrum between 200 and 393 keV, by 1, as all projectiles are charged, and finally with the efficiency of 0.03 averaged over the respective energy interval. We get 0.9×10^{-6} protons/projectile. These protons are practically not influenced by the electric field and hence yield the undistorted blocking pattern. (ii) Positively charged, low energy projectiles, i.e., protons with energies <1 keV (40×10^{-6} protons/projectile). They are accelerated toward the PSD and hence are detected with maximum efficiency of $\approx 85\%$. They produce a distorted pattern that is determined by the electric field and is completely dissimilar to a blocking pattern (e.g., in our geometry a small square is formed). (iii) Positively charged, sputtered W^+ ions (15×10^{-6} W^+ ions/projectile). They behave similarly to low energy protons, i.e., their impact pattern does not at all reflect blocking (our result is a wormlike intensity distribution split at one end). (iv) Protons with 1 keV$<E<10$ keV (3×10^{-6} protons/projectile) con-

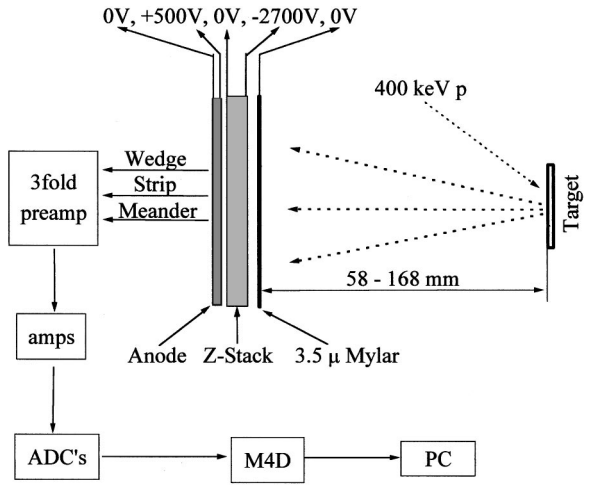

FIG. 2. Side view of the two-dimensional position sensitive detector.

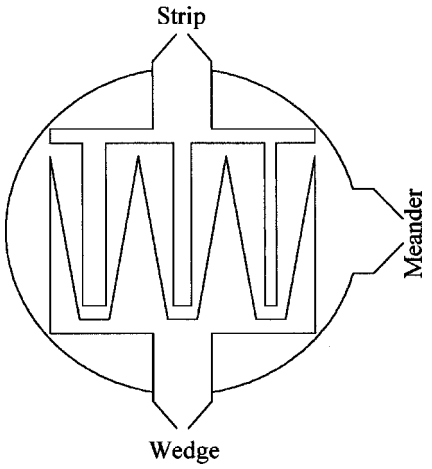

FIG. 3. Sketch of the wedge and strip anodes. Meander is called the residual area in between.

tribute to item (ii). We treat them separately as only a fraction of backscattered protons is focused onto the PSD. (v) The rest of the particles that are detected are subsumed under this item. They produce a more or less uniform background. We summarize: The probability for a projectile to contribute to a clear blocking pattern (0.9×10^{-6}) is only 1.6% of the probability to contribute to a distorted pattern (58×10^{-6}). To get rid of that part of the image, all low energy particles have to be absorbed by a foil.

The usual idea of inserting a grid[15] or a foil[16] in front of the PSD is to increase the MCP efficiency: On the one hand, secondary electrons from the interchannel web of the MCP are repelled and, on the other hand, electrons knocked out of the foil by projectiles are accelerated onto the MCP, thus raising its overall efficiency. Evidently, the foil has to be negatively charged with respect to the PSD, just the opposite of our case. The purpose of our foil is quite different: A large fraction of the spectrum at lower energies is absorbed and the energy of the high energy particles is shifted toward regions of high detection efficiency. In contrast to the target, where we had to consider both backscattered and sputtered particles, we can here ignore sputtered particles (in our case Al atoms) in comparison to the great number of transmitted projectiles.

III. REALIZATION

In Fig. 2 we show the actual arrangement of the detector assembly. At the input side of the detector at a distance of 1 mm we have mounted a 3.5 μm stopping foil made from Mylar®, both sides covered with a thin Al layer. The total thickness has been chosen to stop protons with energies less than 320 keV. The three MCPs are selected for equal resistance so that the voltage drop across each MCP is about the same. They have an active diameter of 45 mm and a thickness of 1 mm. The electrons exiting the third MCP are accelerated by 500 V toward a germanium layer on a 2-mm-thick ceramic substrate. On the rear surface of the ceramic a wedge-and-strip anode is applied (see Fig. 3). The structure of the anode is rather coarse. Hence, the signal of the electrons leaving the last MCP has to be spread out over more than one period of this structure to give a smooth dependence of the electronic signals on impact position. In part this is achieved by the acceleration gap between MCP and germanium anode where the electron cloud expands and in part by the capacitive coupling between the intermediate germanium anode and the WS anode. By optimization of these parameters the spatial resolution can be as small as 60 μm. To suppress the large background due to electrons released at the rim of the detector by spikes of the electric fields, we reduced the active area of the MCP to 41.5 mm.

The position of the detected particles is encoded by charge sensitive amplifiers connected to the wedge (W), strip (S), and (in between) the meander (M) contacts of the anode (Fig. 3) and can be easily transformed from the digitized signals into Cartesian coordinates (x,y) by the following algorithm:[17,18]

$$x=2\mathrm{S}/(\mathrm{W}+\mathrm{S}+\mathrm{M}), \quad y=2\mathrm{W}/(\mathrm{W}+\mathrm{S}+\mathrm{M}). \tag{2}$$

The center of the PSD is positioned in the horizontal plane at a scattering angle of 135° relative to the incoming beam. The detector is mounted on a linear feedthrough in radial direction to vary its solid angle. In stand-by position, the detector is drawn back from the target and can be covered by a shield. The whole system is built on a CF100 flange and can be removed as a whole. The entire detector is bakable up to 523 K.

A Roentdek 4 kV dual power supply provides the bias voltages. The anode structure is floating but could be operated with any appropriate voltage via the threefold charge sensitive Roentdek preamplifier. The outputs of the amplifiers are connected to three Ortec 472A spectroscopy amplifiers and fed further into three Canberra ADCs 8701 (Wilkinson type). Our M4D list mode recording system,[19] mounted on a board to be inserted into a PC, reads the digitized signals and writes them together with the ADC number, corresponding to S, W, and M, and the time of occurrence on hard disk. The intrinsic time resolution is 100 ns. By this, one can off-line select coherent events of the three ADCs by any arbitrary coincidence condition. The performance of the system is restricted by the conversion times of the ADCs and the signal rise time of the preamplifiers, so the rate has to be

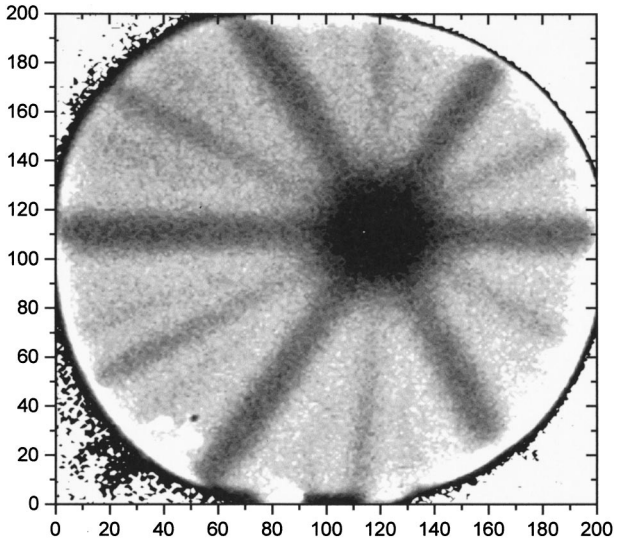

FIG. 4. Blocking pattern of 400 keV protons (called protonogram) onto tungsten with a (111) plane almost parallel to the detector surface. Planes with indices up to (321) can be clearly resolved.

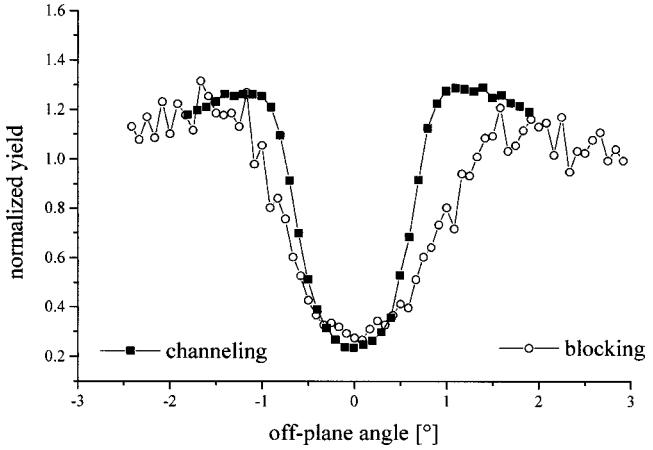

FIG. 5. Comparison of the channeling dip of the (110) plane, as measured in a conventional manner, to the blocking dip derived from the protonogram of Fig. 4.

lower than 10 kHz. The detector itself sets a limit at 50 kHz and the M4D system manages a mean transfer rate of 70 000 events/s and a peak transfer rate of 500 000 events/s. The accidental coincidences of our system are lower than 30 events/s.

In Fig. 4 we show the blocking pattern of 400 keV protons on a tungsten single crystal with a (111) plane almost parallel to the detector. The intersection of the different lines [(110) and (211) planes] corresponds to the $\langle 111 \rangle$ direction. In the lower part on the left-hand side, one can resolve planes with indices up to (321). We have obtained this pattern with the target exposed to a beam of 0.5 nA for 300 s. The resulting list file had a size of 45 Mbytes (!), which was scanned for coincidences and converted into a graphic representation within 50 s using a PC with Intel Pentium MMX 200 MHz processor and standard hard disk. To improve the linearity of the transformation we corrected for the capacative coupling between the anode structures. The resulting image has a (rather arbitrarily chosen) size of 201×201 pixels (646 kbytes).

In Fig. 5 we show a channeling dip together with the corresponding blocking dip as derived from the protonogram of Fig. 4. The width of the channeling dip ($\approx 1°$ or $\pm 0.5°$) is hardly influenced by the divergence of the incoming beam, which is shaped by two collimators of 1.2 and 0.8 mm in diameter, 2450 mm apart; we get a divergence of $\pm 0.023°$. Contrary to channeling, the width of the blocking dip is affected by the divergence of the projectiles coming from the beam spot (2.3 mm diameter) and hitting the detector within a circle corresponding to its spatial resolution. The distance of the PSD from the target is 133 mm. We want to point out that due to multiple angular scattering in the foil an additional spatial resolution $\Delta\rho$ has to be present. Assuming most of the particles leave the target within $\pm 45°$, we have $\Delta\rho \approx \pm 1$ mm. If we neglect for the moment $\Delta\rho$, simply the beam spot is responsible for a divergence of $\pm 0.5°$ which can almost alone be made responsible for the broader blocking dip ($\pm 1.1°$). This can be explained in the following way. Multiple scattering primarily affects slow projectiles. If they are charged they will be immediately directed toward the topmost MCP and hit the MCP close to the nominal impact position. Only if they are neutral will they slightly obscure the pattern, e.g., make the shoulders on both sides of the dip less pronounced.

To get the three angles to feed the execution program of the goniometer we fit straight lines to the major planes by means of a least-squares algorithm. From the intersection of these lines on the image we can calculate the relevant angles. For targets with slanted front and back surfaces a second protonogram taken under an azimuthal rotation of 180° gives the correct position. With the known orientation of a test crystal fixed by conservative methods we could determine the dispersion of the image: in the case of Fig. 5 there are 12.3 pixels per degree.

In summary, we are now able to adjust the angular position of each crystal with an accuracy of $+/-0.09°$. Meanwhile, this two-dimensional position sensitive detector has become a standard device in our target chamber where investigations of single crystals by ion scattering are routinely carried through.

ACKNOWLEDGMENTS

One of us (D.S.) acknowledges the aid of P. Radl during these investigations. This work has been supported by the ''Jubilaeumsfonds der Oesterreichischen Nationalbank'' under Contract No. 6778.

[1] J. Lindhard, Mat.-Fys. Medd. Dan. Vid. Selsk. **34**, No. 14 (1965).
[2] H. Ellmer, W. Fischer, A. Klose, and D. Semrad, Rev. Sci. Instrum. **67**, 1794 (1996).
[3] E. Laegsgaard, Nucl. Instrum. Methods **162**, 93 (1979).
[4] M. Morjean *et al.*, Nucl. Phys. A **630**, 200 (1998).
[5] E. H. M. Heijne *et al.*, IEEE Trans. Nucl. Sci. **NS-42**, 413 (1995).
[6] P. Burger (private communication).
[7] S. Dhawan, IEEE Trans. Nucl. Sci. **NS-28**, 672 (1981).
[8] J. L. Wiza, Nucl. Instrum. Methods **162**, 587 (1979).
[9] J. Oberheide, P. Wilhelms, and M. Zimmer, Meas. Sci. Technol. **8**, 351 (1997).
[10] J. Vukanic and P. Sigmund, Appl. Phys. **11**, 265 (1976).

[11] W.-K. Chu, J. W. Mayer, and M. A. Nicolet, *Backscattering Spectrometry* (Academic, New York, 1978), p. 72.
[12] U. Littmard and S. Fedder, Nucl. Instrum. Methods **194**, 607 (1982).
[13] J. Roth, J. Bohdansky, and W. Ottenberger, Max-Planck-Institut für Plasmaphysik, IPP 9/26, 1979.
[14] K. H. Berkner, I. Bornstein, R. V. Pyle, and J. W. Stearns, Phys. Rev. A **6**, 278 (1972).
[15] H. O. Funsten, D. M. Suszcynsky, R. W. Harper, J. E. Nordholt, and B. L. Barraclough, Rev. Sci. Instrum. **67**, 145 (1996).
[16] P. V. Schmidt *et al.*, Nucl. Instrum. Methods Phys. Res. A **376**, 139 (1996).
[17] H. O. Anger, IEEE Trans. Nucl. Sci. **NS-13**, 380 (1966).
[18] C. Martin, P. Jelinsky, M. Lampton, R. F. Malina, and H. O. Anger, Rev. Sci. Instrum. **52**, 1067 (1981).
[19] R. Wordel, D. Mouchel, E. Steinbauer, and R. Oyrer, Int. J. Appl. Radiat. Isot. **47**, 1061 (1996). More information on the M4D system may be obtained from E. Steinbauer, stein@exphys.uni-linz.ac.at